THE JOURNAL OF PHYSICAL CHEMISTRY B

Article

pubs.acs.org/JPCB

A New Class of Purple Membrane Variants for the Construction of Highly Oriented Membrane Assemblies on the Basis of Noncovalent Interactions

Roelf-Peter Baumann,[†] Annegret P. Busch,[†] Björn Heidel,[‡] and Norbert Hampp*[,†]

[†]Philipps University of Marburg, Department of Chemistry, Hans-Meerwein-Str., Bldg. H, D-35032, Germany

[‡]Universität Siegen, Fak.IV/Dept. Chemistry-Biology, Adolf-Reichwein-Str. 2, D-57068, Germany

Supporting Information

ABSTRACT: Purple membranes (PM) from *Halobacterium salinarum* have been discussed for several technical applications. These ideas started just several years after its discovery. The biological function of bacteriorhodopsin (BR), the only protein in PM, is the light-driven proton translocation across the membrane thereby converting light energy into chemical energy. The astonishing physicochemical robustness of this molecular assembly and the ease of its isolation triggered ideas for technical uses. All basic molecular functions of BR, that is, photochromism, photoelectrism, and proton pumping, are key elements for technical applications like optical data processing and data storage, ultrafast light detection and processing, and direct utilization of sunlight in adenosine 5′-triphospate (ATP) generation or seawater desalination. In spite of the efforts of several research groups worldwide, which confirmed the proof-of-principle for all these potential applications, only the photochromism-based applications have reached a technical level. The physical reason for this is that no fixation or orientation of the PMs is required. The situation is quite different for photoelectrism and proton pumping where the macroscopic orientation of PMs is a prerequisite. For proton pumping, in addition, the formation of artificial membranes which prevent passive proton leakage is necessary. In this manuscript, we describe a new class of PM variants with oppositely charged membrane sides which enable an almost 100% orientation on a surface, which is the key element for photoelectric applications of BR. As an example, the mutated BR, BR-E234R7, was prepared and analyzed. A nearly 100% self-orientation on mica was obtained.

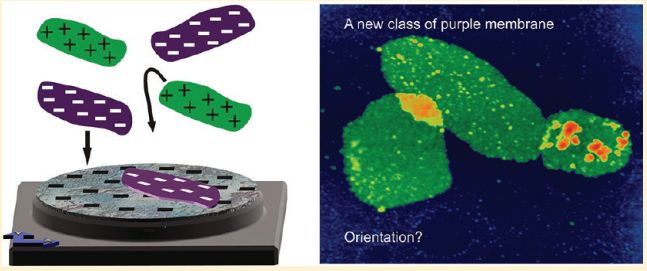

INTRODUCTION

Its interesting properties make the paradigm membrane protein bacteriorhodopsin (BR) from *Halobacterium salinarum* a promising material for technical applications in nanobiotechnology.[1−6] Within the so-called purple membrane (PM) comprising bacteriorhodopsin and lipids only,[7,8] BR is arranged in trimers forming a hexagonal two-dimensional crystalline lattice of enormous stability.[9] Structurally, bacteriorhodopsin features seven α-helical domains, which are interconnected by extramembraneous loops and which enclose a binding pocket for the retinylidene chromophore bound to lysine 216 via a Schiff-base linkage. The intricate, well-studied photocycle[10,11] of BR provides for a vectorial proton translocation mechanism[12] while associated shape and color changes are responsible for the interesting photooptic and photoelectronic properties.

Although BR and PM have been intensively studied over the past three decades bringing forth numerous proposed technical applications, some of which have been successfully demonstrated in a lab environment, no commercial products are available yet. The various bacteriorhodopsin properties being exploited in more sophisticated implementations are of a vectorial nature, that is, their magnitude or effect critically depends on the orientation of the protein and on the PM and may be amplified or dampened by a high degree or a low degree of PM orientation, respectively. For example, a photovoltage of up to 250 mV may be generated across a single PM layer by charge separation upon illumination.[13] In a highly oriented stack of PMs, where every layer is oriented in the same direction, this potential may be dramatically increased, while counteroriented PMs result in a decrease in net potential. Besides possible photoelectric applications, light- and pH-dependent bending of PMs is of interest to the field of biosensors.[14,15] Further, BR within PM may serve as a nanoscaled template for nano-bio hybrid structures by providing spatially highly ordered binding sites again in dependence on the orientation of PM. An important prerequisite for many applications is thus a high degree of orientation of PM patches both laterally and vertically, which is difficult to achieve especially on a large scale.

Several different approaches to realize a high degree of PM orientation have been explored in the past with varying degrees of success. Both membrane sides naturally feature a distinct, pH-dependent charge in aqueous suspension, which may be

Received: November 10, 2011
Revised: January 26, 2012
Published: March 15, 2012

exploited for orientation purposes. Considering, for example, layer-by-layer (LBL) techniques, this promises to be a simple and elegant way to assemble various homogeneous as well as heterogeneous PM structural architectures. However, the cytoplasmic (CP) and extracellular (EC) sides are both negatively charged in solution with the CP side being only slightly more negative. This provides for a preferred adsorption of one side over the other to a given positively or negatively charged surface but does not yield a high degree of orientation in particular because the difference in charge of both sides is further weakened by the adsorption of cations. Oppositely charged membrane surfaces would alleviate these problems. Electric field sedimentation (EFS) also tries to exploit the difference in charge or rather in the resulting dipole moment to preorient PMs in solution by means of an electric field prior to adsorption.[16] Again, the small difference in charge of both sides is a disadvantage as well as the large average size of PM patches of about 1 μm, which hinders rotation and even prevents Brownian motion. Further approaches utilize Langmuir–Blodgett (LB) deposition,[17] where PMs are finely dispersed at the air–water interface, sol–gel encapsulation,[18] and using polymers as immobilization matrices.[19] In most cases, PM orientation is only indirectly induced and deduced on the basis of the direction and intensity of the photoelectric response of the prepared PM mono- or multilayers after they have been incorporated into a device system. The only dependable direct system to allow a perfect orientation of bacteriorhodopsin wild-type (BR-WT) and a highly accurate determination of the ratio of orientation of PM sheets thus far is the antibody-mediated orientation of PMs in combination with immunogold labeling.[20] This technique, however, is not suitable for more than the laboratory production scale as it is rather delicate, costly, and time demanding. Further, such PM assemblies utilizing antibodies as supporting material are not very stable from a thermodynamic point of view and will thus be limited in their potential use for technical applications.

Genetic engineering of bacteriorhodopsin variants has become routine and allows for BR to be specifically tailored toward application needs. Variants that feature specific binding sites such as BR-Q3C and BR-D96C where glutamine and aspartic acid, respectively, are replaced by cysteine have been synthesized and have been shown to covalently bind to a gold substrate.[21,22] This approach is especially interesting to applications based on the photoelectrism properties of bacteriorhodopsin. To exploit such specifically functionalized variants to achieve a high degree of membrane orientation, however, still presents inherent limitations with respect to the range of substrates that can be used and of course the reversibility of the adsorption process. Although irreversible bonding makes PM patches and consequently PM assemblies more robust, they will inevitably lack the ability to change as their degrees of freedom and their dynamics are limited. In contrast, a noncovalent approach to PM orientation and assembly of more complex architectures is reversible and sensitive to the environment entailing both adaptivity and stimuli-responsiveness to achieve facile fabrication and functional versatility.

We present a novel approach by utilizing genetic modification of bacteriorhodopsin wild-type to reverse the charge of one entire PM side. By enhancing noncovalent interactions in this manner, adsorption and orientation will be charge- and dipole-moment mediated thus allowing for a broad range of substrates to be used while maintaining complete reversibility of the process. To change the charge on one entire membrane side, seven arginines were inserted into the C-terminal part of the amino acid sequence resulting in the formation of BR-E234R7 featuring a positively charged cytoplasmic side. Tapping mode atomic force microscopy (TM-AFM) and electrostatic force microscopy (EFM) were utilized for side differentiation, charge, and orientation analysis.

EXPERIMENTAL METHODS

Materials. *$SNOB_{Marburg}$.* After the transformation of the deletion vector pROB in *Halobacterium salinarum* strain S9 and following growth on mevinoline containing plates, single purple colonies were selected which carry the mevinoline resistance gene (Mev^r) within the deletion cascade. Because pROB does not replicate autonomously (missing origin for replication for *Halobacterium salinarum*, ori^-) but recombines only homologously, all positive transformants possess both deletion cascade and bacterioopsin wild-type gene (*bop*). Individual selected colonies were inoculated in aqueous medium without mevinoline. After multiple inoculations, several aliquots were incubated on full medium plates from which individual none purple colonies were transferred to full medium plates with and without mevinoline. Clones that had lost the resistance cascade and could thus only survive on plates without mevinoline were picked and inoculated in aqueous medium. The establishment of $SNOB_{Marburg}$ was verified by genomic DNA preparation and PCR testing.

pUS-Mev-bop-$arg_{(7)}$. The *pUS-Mev-bop-$arg_{(7)}$* construct was generated by directed mutagenesis of the bacterioopsin gene (*bop*) utilizing *pUS-Mev* and Phusion Hot Start High-Fidelity DNA Polymerase. The first PCR step was performed with the following primer pairs: IF-*Bam*HIseq and $arg_{(7)}$*AvrII*rev, and IF-*Hin*dIIIrev and $arg_{(7)}$*Nde*Iseq. $arg_{(7)}$*Nde*Iseq and $arg_{(7)}$*AvrII*rev contain the nucleotide sequence encoding for the seven arginies to be inserted into the C-terminal part of BOP. Both PCR products were purified via DNA gel and were used as templates for a second flanked primer extension (IF-*Bam*HIseq and IF-*Hin*dIIIrev). The amplified final product was recombined into the target suicide vector *pUS-Mev* by the In-Fusion advantage PCR cloning kit.

AFM/EFM Sample Substrates. Mica substrates used in AFM/EFM experiments were purchased from Plano GmbH, Wetzlar, Germany, as were highly oriented pyrolytic graphite (HOPG) substrates. Both substrates were freshly cleaved before use.

Methods. *Ultracentrifugation.* For isolation of PM, a four-phase sucrose density gradient was used. Eighty milliliters of (D+)-sucrose solutions (Acros Organics) of concentrations 34%, 36.5%, 38%, 41%, and 44% was prepared and was checked for the correct refractive index. From highest to lowest density, 4.6 mL of each solution was funneled into an ultracentrifugation vial (38.5 mL; Kontron 9091-90200) via a peristaltic pump to form separate layers. Five milliliters of raw PM material (OD 20) was placed on the sucrose density gradient and was tared with distilled water. In the case of a deviating OD, the mass of raw PM material must be equivalent to the mass of 5 mL of OD = 20. The tared buckets (Kontron Instruments AG) were centrifuged in a T-1080 Kontron Instruments AG with TST 28-38 rotor at 4 °C and 25 000 rpm for 19 h. The yellowish supernatant and redish cell remnants were cast away. The PM phase was carefully pipetted into six ultracentrifugation vials, which were filled with distilled water, were tared, and were centrifuged again at 4 °C and 25 000 rpm for 2.5 h. To wash the resulting pellets, the supernatant was cast away and the pellets were distributed in eight Sorvall centrifugation

dx.doi.org/10.1021/jp210825x | J. Phys. Chem. B 2012, 116, 4134–4140

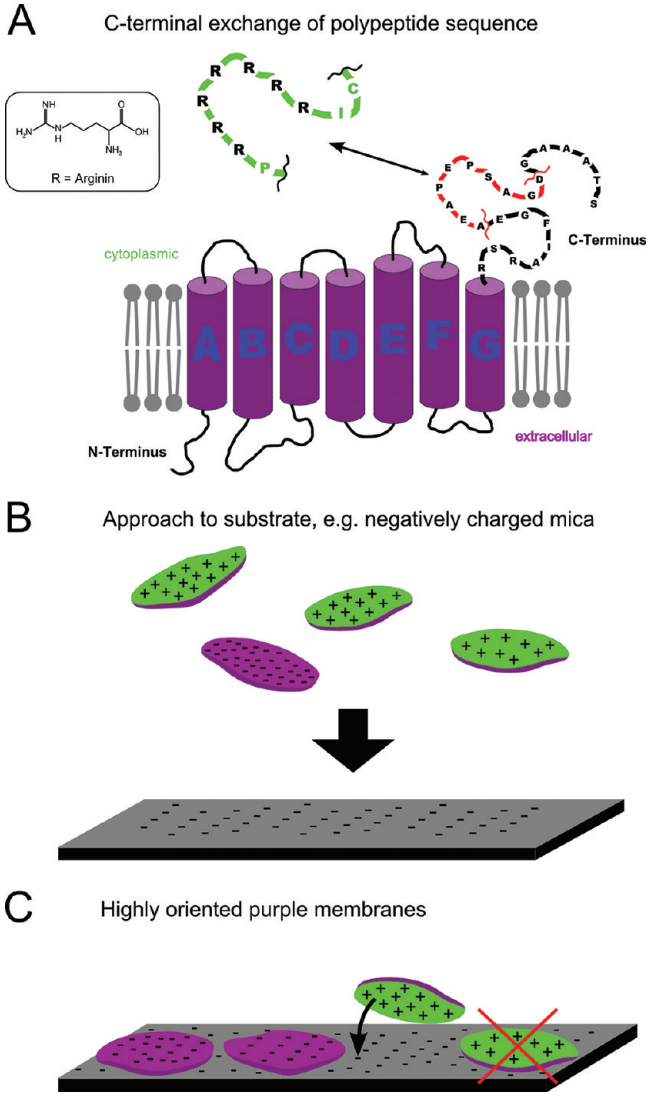

Figure 1. Genetic modification of bacteriorhodopsin leads to PM adsorption in a highly oriented fashion. (A) C-terminal exchange of a short polypeptide sequence (red) by seven arginines (green) renders the former negatively charged cytoplasmic side of PM positive. (B) Both sides of PM-E234R7 are oppositely charged, which leads to an orientation effect upon substrate approach. (C) On negatively charged mica, PM-E234R7 selectively adsorbs with the positively charged cytoplasmic side only resulting in highly oriented PM patches.

vials (Nalgene), were filled with distilled water, and were mixed with 1 mL phosphate buffer (0.06 M, pH 6.8) each prior to centrifugation in the Sorvall centrifuge at 20 °C and 18 500 rpm for 25 min. This washing step was repeated once more before the supernatant was cast away, and the remaining pellets were combined with a little distilled water in one flask (Kautex).

Mass Spectrometry. Samples were prepared according to Hufnagel et al.[23] Twenty nanomoles of PM was suspended in 1 mL ethanol in an Eppendorf cup, was vortexed for 2 min, and was sonicated (Ultrasound disintegrator Sonifier II, Branson, United Kingdom; 1 s pulse, 5 s pulse off, with an amplitude of 25%, 5 s time). The addition of 500 μL hexane was followed by differential centrifugation for 3 min at 3000*g* at room temperature. The supernatant was discarded, and 1 mL hexane was added. The sample was vortexed and was treated again with ultrasound according to the aforementioned conditions. The supernatant was again discarded, and the remaining white colored

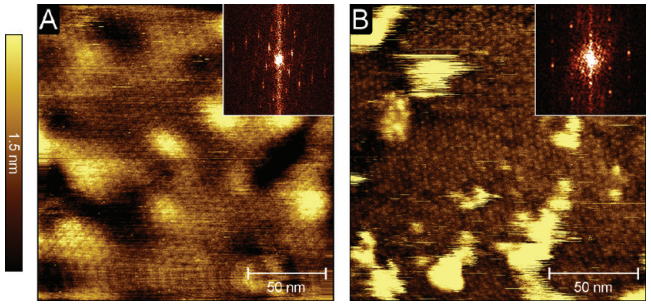

Figure 2. High-resolution TM-AFM height images of PM-E234R7 on HOPG to verify the structural integrity of the hexagonal two-dimensional crystalline BR assembly. (A) The characteristically donut-shaped cytoplasmic side of a PM-E234R7 patch. (B) The triangular-shaped extracellular side of a different PM-E234R7 patch. Respective insets of the Fourier transform show the hexagonal lattice.

pellet was dried in air for 15 min. The pellet was dissolved in a solvent mixture comprising 200 μL chloroform, 200 μL methanol, 175 μL distilled water, and 10 μL methanoic acid.

Mass spectrometry (MS) was performed on a Qstar Pulsar I mass spectrometer (Applied Biosystems, Darmstadt, Germany) equipped with an electrospray ionization source (ESI). Samples were continuously injected via Hamilton syringe with a flow rate of 25 μL/min. ESI parameters were as follows: Ion spray voltage 5 kV, declustering potential (DP1) 80 V, focusing potential (FP) 220 V, declustering potential 2 (DP2) 15 V. The parameters for ionization (N_2) and protective gas (N_2) were 25. For deconvolution purposes, the Bayesian Protein Reconstruct tool as part of the BioAnalyst 1.1.5 software package was used. Measurements were performed in positive mode.

UV/vis. Absorption characteristics of BR samples were analyzed using a lambda35 photospectrometer from Perkin-Elmer. To determine the absolute concentrations of PM containing samples, optical scattering effects must be taken into account. Because of varying PM size, background scattering is not constant and may not be eliminated from the recorded absorption by mathematical means. To alleviate this problem, sufficiently homogenized samples were always analyzed in the light-adapted B intermediate of the protein at 570 nm, and a linear correction of the background scattering at 800 nm to optical density (OD) = 0 was performed. The coefficient of extinction of the B intermediate of BR used is 62 700 mol^{-1} cm^{-1}. Samples containing 20 μL PM suspension in 980 μL Millipore water were measured against a reference sample of 980 μL Millipore water.

AFM/EFM. Tapping-mode atomic force microscopy (TM-AFM) was chosen for imaging in order to minimize interaction forces, especially sheer, between tip and sample. Imaging was performed in liquid on a Nanoscope IV system (Veeco, Santa Barbara, CA). All images were measured using TM-AFM with constant amplitude attenuation. The cantilever approach was performed with an initial drive amplitude of 250 mV (tip oscillation amplitude 1−2 V). Once the tip had engaged, both drive amplitude and set point were adjusted to the minimal forces possible.

Electrostatic force microscopy (EFM) measurements were conducted in air using SCM-PIT tips (antimony (n) doped Si, k = 1−5 N/m, f_0 = 70−83 kHz, 0.01−0.025 Ω/cm, Veeco, Santa Barbara, CA, United States) utilizing the Nanoscope's LiftMode feature. This mode of surface potential detection is a two-pass procedure in which the surface topography is obtained

dx.doi.org/10.1021/jp210825x | J. Phys. Chem. B 2012, 116, 4134−4140

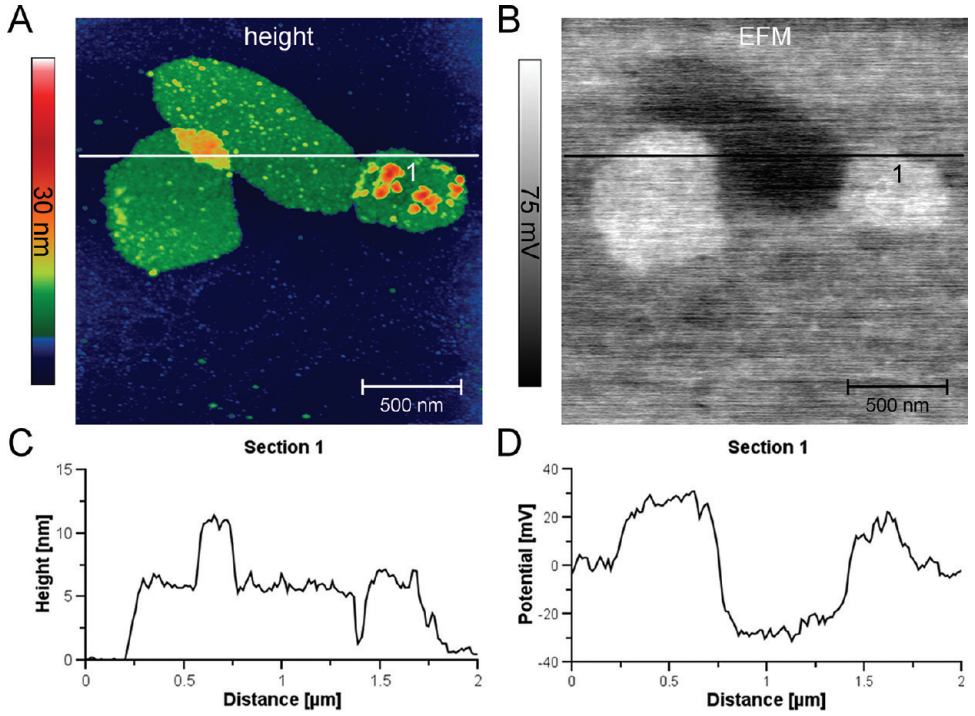

Figure 3. EFM study of PM-E234R7 on HOPG confirms the successful genetic modification of bacteriorhodopsin and consequent charge reversal of the cytoplasmic side of PM. (A) The TM-AFM height image reveals three PM-E234R7 patches flatly adsorbed to HOPG featuring an ordinary wild-type-like membrane topology (C). (B) In the corresponding EFM image, two positively charged patches and one negatively charged PM species are observed, which face cytoplasmic and extracellular side up, respectively. (D) The corresponding section reveals a potential difference between both membrane sides of about 60 mV.

by standard tapping mode in the first pass, and the surface potential is measured on the second pass. Just before the second pass, the tip is moved to a configurable lift height above the sample surface. On the second pass of each line, the tip is then moved at a constant height, tracing the topography that was recorded in the first pass. The two measurements are thus interleaved, that is, they are each measured one line at a time.

PM stock solutions of both variant and wild-type were diluted in a 150 mM KCl, 10 mM Tris-HCl, pH 8.2 buffer to a final absorbance (OD) of 0.2−0.3 at 570 nm. Fifty microliters of imaging buffer (300 mM KCl, 10 mM Tris-HCl, pH 7.8) was pipetted together with 5−10 μL of the PM suspension onto 1 × 1 cm substrate pieces of mica or HOPG, respectively. After 10−20 min of incubation, excess material was removed by extensive rinsing with imaging buffer (10 × 20 μL). Non-EFM analysis was performed in liquid. For this, samples were mounted onto the sample stage where they were allowed to stand for 30 min before imaging in order to reach thermal equilibrium. Samples for EFM measurements were carefully dried in air or argon stream and were measured immediately once mounted onto the sample stage.

All AFM experiments were conducted at room temperature (21 °C).

RESULTS AND DISCUSSION

Halobacterium salinarum has been established as a model organism for the investigation of various biological processes.[24] This is especially true for the expression and regulation on the genetic and protein level.[25,26] Genetic modification of bacteriorhodopsin is well established, and a multitude of direct point-mutations of BR and their overexpression allowed us to investigate and elucidate the role of various amino acid moieties as intermediates in the catalytic and vectorial proton translocation over the course of the BR photocycle.[27−29] Genetic modification of the bacterioopsin gene (BOP) also allowed for structural and dynamic interactions between lipids and helices and for intrahelical interactions between specific monomers as well as orientation of amino acid side chains to be studied. Considering the desired charge reversal of one entire PM side, genetic modification of BOP bares the great advantage over chemical modification that all proteins are derivatized by the mutation without exception. Further, the modification of the extramembraneous C-terminal loop should not affect or alter the photooptic or photoelectric properties of BR-E234R7. To change the charge of the cytoplasmic membrane side to achieve a high degree of orientation of PM at the solid−liquid junction, genetic modification was used as illustrated in Figure 1.

According to the side chain pK_a, the guanidinium residues of the arginine moieties should be protonated and should lead to an overall positive charge of the cytoplasmic side of the resulting PM-E234R7 under virtually all desirable environmental conditions. Enhancing the charge difference between both membrane sides and especially reversing the charge of one side completely should consequently increase orientation and provide for a substrate-dependent control of orientation. For the creation of the bacterioopsin (BOP) mutant, the 1993 introduced homologous expression system was used.[30] The BOP deficient strain SNOB (S nine without BOP)[31] was transformed with a mutated *bop* shuttle-vector *pUS-Mev-bop-arg*$_{(7)}$. To pre-empt genetic mutation of the *bop*-gene-cluster and to exclude cross-contamination, SNOB was reestablished ($SNOB_{Marburg}$) according to the homologous recombination procedure by Pfeiffer.[31] Separation of the modified PM (PM-E234R7) from red membrane and cellular components after

dx.doi.org/10.1021/jp210825x | J. Phys. Chem. B 2012, 116, 4134−4140

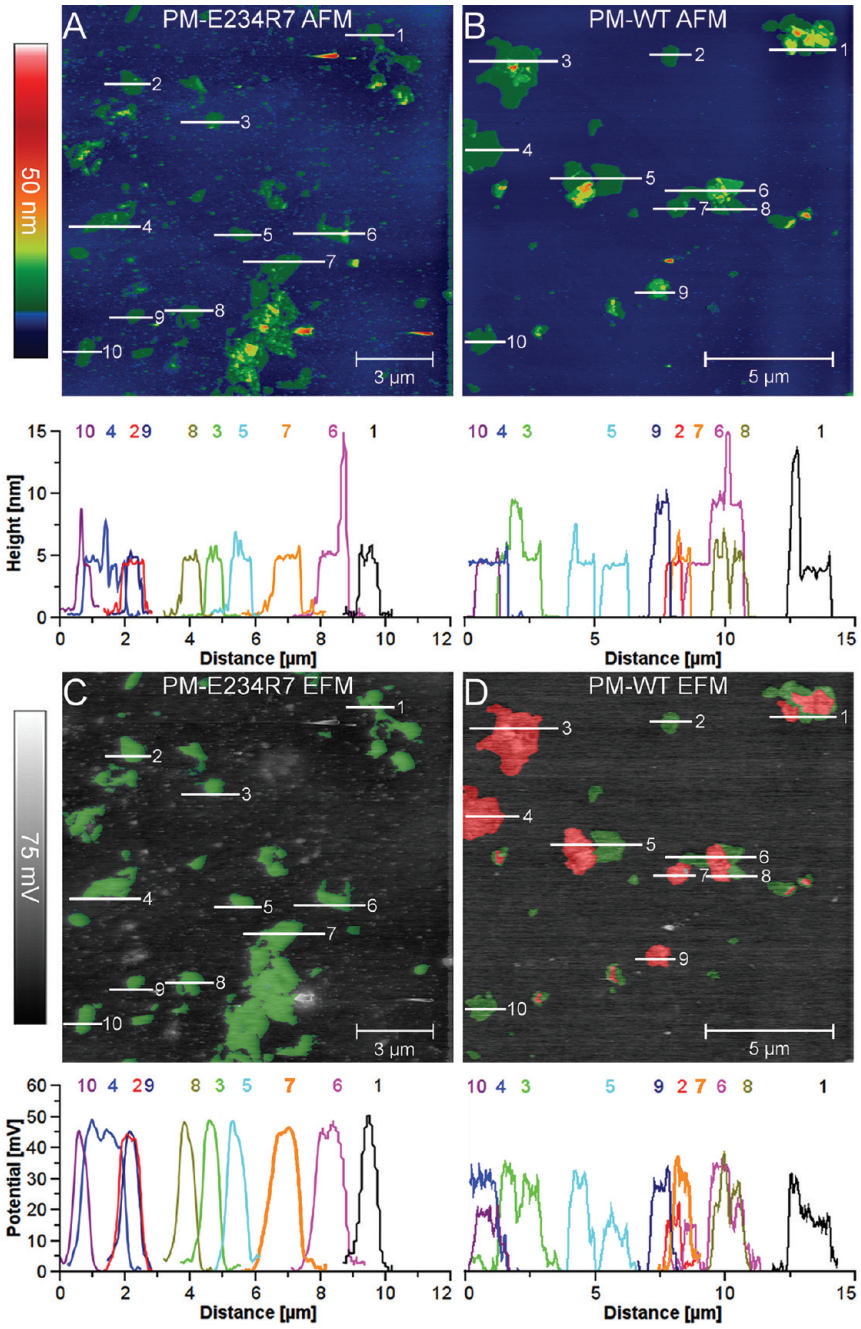

Figure 4. EFM analysis of PM-E234R7 (left column) on mica in comparison to PM-WT (right column) reveals highly oriented PM patches. (A, B) TM-AFM images with corresponding sections compare and contrast PM-E234R7 and PM-WT showing that membrane topology remains unaltered by the genetic modification. (C, D) EFM analysis reveals that PM-E234R7 patches are highly oriented according to their surface potential. To guide the reader's eye, membrane patches featuring the same surface potential relative to the mica background have been highlighted with the same color. Blue and green patches face extracellular side up, and red-colored patches face cytoplasmic side up. While PM-WT still features both CP and EC sides, PM-E234R7 selectively adsorbs with the CP side to mica only as the corresponding sections show.

cell rupture by osmotic shock via dialysis was performed over a four-phase sucrose density gradient. As the genetic modification results in an increase in mass of BR-E234R7 by about 1.8% with respect to BR-WT, the observed buoyant density of PM-E234R7 is slightly greater than the wild-type reference of ρ = 1.18 g cm^{-3}, and consequently, PM-E234R7 is found further down on the sucrose density gradient (Figure 1 of the Supporting Information). Mass spectroscopy (Figure 2 of the Supporting Information) provides a mass of 27281 Da for BR-E234R7 corresponding well with the theoretical value of 27283.3 Da. Absorption characteristics of the E234R7 variant fully resemble the wild-type according to UV/vis analysis (Figure 3 of the Supporting Information). As was expected, the introduction of seven arginines on the cytoplasmic side of the membrane protein has no effect on the absorption spectrum and photooptic properties of BR. The structural integrity of the hexagonal crystalline assembly upon genetic modification was verified by high-resolution tapping-mode atomic force microscopy (TM-AFM) on highly oriented pyrolytic graphite (HOPG). Because grounded HOPG samples are uncharged,

dx.doi.org/10.1021/jp210825x | J. Phys. Chem. B 2012, 116, 4134–4140

PM-E234R7 will adsorb unspecifically with either CP or EC side to it. This allows for the donut-shaped hexagonal lattice of the cytoplasmic and the triangular-shaped hexagonal lattice of the extracellular side to be resolved as seen in Figure 2A and B, respectively.

According to Figure 2, genetic modification influences neither the crystalline structure nor the lattice assembly of the variant PM-E234R7.

To analyze PM-E234R7 surface potential to probe for the postulated charge reversal, electrostatic force microscopy (EFM) was utilized.

Figure 3 shows TM-AFM and the corresponding EFM image of PM patches of variant E234R7 adsorbed onto highly oriented pyrolytic graphite. HOPG samples were grounded in order to achieve a defined reference potential for EFM measurements. The variants morphology and topology corresponds to the wild-type and features average patch sizes of about 1 μm with a height of 5 nm (compare Figure 3C). EFM analysis reveals that the three imaged membranes feature two distinct surface potentials of about 30 mV and −30 mV relative to the HOPG substrate surface background. According to Knapp et al.,[32] wild-type PMs feature surface potentials relative to a grounded HOPG background of about −20 mV for the more negative extracellular and −10 mV for the less negative cytoplasmic side. The more negative patch in the middle thus faces extracellular side up, while the left and the right patches face cytoplasmic side up. Interestingly, the charge on the cytoplasmic side is not just less negative than on the extracellular for PM-E234R7 as is also the case for the wild-type but is indeed positive relative to the grounded HOPG background indicating that the charge reversal by genetic engineering was successful. On the electrostatically neutral HOPG substrate surface, PM-E234R7 apparently assumes no specific orientation and adsorbs equally well with the EC and CP side. A different picture develops for negatively charged mica as a substrate.

Figure 4 shows TM-AFM and the corresponding EFM images with sections of selected membranes of PM-E234R7 (left column) in comparison to PM-WT (right column). Again, from the height images (A and B), no discernible difference in morphology and topology between both wild-type and variant becomes evident. Most membranes feature heights of 5 nm although some membrane stacks with heights of a multiple of 5 nm, that is, 10 and 15 nm, are observed in the corresponding sections for the PM-WT reference. EFM images C and D, however, clearly reveal a high degree of orientation of the variant on mica in comparison to the wild-type. Sections of selected PM patches feature only one potential of about 45 mV relative to the mica substrate in the case of PM-E234R7. All membranes must thus be oriented such that the same side faces upward. Although an absolute assessment of the electric field distribution is not possible in this specific setup because of the insulating nature of the mica substrate, it is obvious that PM-E234R7 adsorbs with the modified and positively charged CP side to the negatively charged mica substrate, and consequently, the membrane side observed is the extracellular. In the wild-type reference, on the contrary, two different potentials emerge from sections of selected PM patches. Observed potentials are about 20 mV and 30 mV relative to the mica background. Again, because of the insulating nature of mica, no absolute assessment is possible, but relative estimations can still be performed with high accuracy. Similar to the measurements on HOPG, the potential of both PM sides differs in agreement with literature by about 10 mV.[32] The more negative (20 mV, green) patches can thus be attributed to the extracellular, while the less negative (30 mV, red) ones can be attributed to the cytoplasmic side. In contrast to the highly oriented PM-E234R7, PM-WT on mica does not possess a preferential side of adsorption.

CONCLUSIONS

By means of genetic modification of bacterioopsin and homologous expression in *H. salinarum*, we were able to create a crystalline PM with a strong dipole moment. The general concept we established and followed to achieve this was to replace several amino acids in the C-terminal part of bacteriorhodopsin with positively charged ones in order to accumulate enough positive charges on the intracellular side of PM and by doing so to cause a charge reversal of this side. From the pool of amino acids compatible with our theory, we chose to insert seven arginines which resulted in the desired overall charge reversal of the cytoplasmic side of PM because of their pH indifferent positively charged guanidinium moiety. EFM proved to be a valuable tool to verify the introduced charge reversal on the PM level and congruently enabled us to analyze the resulting high degree of orientation of PM-E234R7 obtained on mica. The results presented are not only interesting from a scientific point of view but bare significant importance for all technical applications where a high degree of membrane orientation is required. Further, the oppositely charged membrane sides of PM-E234R7 in combination with layer-by-layer techniques should allow for an easy construction even of sophisticated PM structural architectures.

ASSOCIATED CONTENT

Supporting Information

Ultracentrifugation sucrose density gradients, SDS page plot, mass, UV−vis of PM-E234R7/BR-E234R7, AFM high-resolution height image of PM-E234R7 on mica. This material is available free of charge via the Internet at http://pubs.acs.org.

AUTHOR INFORMATION

Corresponding Author

*Fax: +49 6421 2825798. Tel: +49 6421 2825775. E-mail: hampp@staff.uni-marburg.de.

Notes

The authors declare no competing financial interest.

ACKNOWLEDGMENTS

We thank Nina Schromczyk for the preparation and purification of PM-E234R7.

REFERENCES

(1) Hampp, N. *Chem. Rev.* **2000**, *100*, 1755−1776.
(2) Jin, Y.; Honig, T.; Ron, I.; Friedman, N.; Sheves, M.; Cahen, D. *Chem. Soc. Rev.* **2008**, *37*, 2422−2432.
(3) Chu, L.-K.; Yen, C.-W.; El-Sayed, M. A. *Biosens. Bioelectron.* **2010**, *26*, 620−626.
(4) Hampp, N.; Bräuchle, C.; Oesterhelt, D. *MRS Bull.* **1992**, *17*, 56−60.
(5) Hampp, N.; Zeisel, D. *IEEE Eng. Med. Biol.* **1994**, *13*, 67−74.
(6) Yao, B.; Ren, Z.; Menke, N.; Wang, Y.; Zheng, Y.; Lei, M.; Chen, G.; Hampp, N. *Appl. Opt.* **2005**, *44*, 7344−7348.
(7) Haupts, U.; Tittor, J.; Oesterhelt, D. *Annu. Rev. Biophys. Biomol. Struct.* **1999**, *28*, 367−399.

(8) Krebs, M. P.; Isenbarger, T. A. *Biochim. Biophys. Acta* **2000**, *1460*, 15−26.
(9) Shen, Y.; Safinya, C. R.; Liang, K. S.; Ruppert, A. F.; Rothschild, K. J. *Nature* **1993**, *366*, 48−50.
(10) Lanyi, J. K. *Annu. Rev. Physiol.* **2004**, *66*, 665−688.
(11) Lanyi, J. K. *Biochim. Biophys. Acta* **2006**, *1757*, 1012−1018.
(12) Subramaniam, S.; Henderson, R. *Nature* **2000**, *406*, 653−657.
(13) Hampp, N.; Oesterhelt, D. *Nanobiotechnology: Concepts, Applications and Perspectives*; Mirkin, C., Niemeyer, C., Eds.; Wiley-VCH: Weinheim, Germany, 2004; pp146−167.
(14) Rhinow, D.; Hampp, N. *J. Phys. Chem. B* **2008**, *112*, 13116−13120.
(15) Baumann, R.-P.; Schranz, M.; Hampp, N. *Phys. Chem. Chem. Phys.* **2010**, *12*, 4329−4335.
(16) Keszthelyi, L. *Biochim. Biophys. Acta* **1980**, *598*, 429−436.
(17) Miyasaka, T.; Koyama, K. *Thin Solid Films* **1992**, *210/211*, 146−149.
(18) Chen, Z.; Lewis, A.; Takei, H.; Nebenzahl, I. *Appl. Opt.* **1991**, *30*, 5188−5196.
(19) Wu, S.; Ellerby, L. M.; Cohan, J. S.; Dunn, B.; El-Sayed, M. A.; Valentine, J. S.; Zink, J. I. *Chem. Mater.* **1993**, *5*, 115−120.
(20) Koyama, K.; Yamaguchi, N.; Miyasaka, T . *Science* **1994**, *265*, 762−765.
(21) Schranz, M.; Noll, F.; Hampp, N. *Langmuir* **2007**, *23*, 11134−11138.
(22) Wu, A.; Jia, Z.; Schaper, A.; Noll, F.; Hampp, N. *Langmuir* **2006**, *22*, 5213−5216.
(23) Hufnagel, P.; Schweiger, U.; Eckerskorn, C.; Oesterhelt, D. *Anal. Biochem.* **1996**, *243*, 46−54.
(24) Soppa, J. *Microbiology* **2006**, *152*, 585−590.
(25) Soppa, J. *Mol. Microbiol.* **1999**, *31*, 1295−1305.
(26) Soppa, J. *Curr. Opin. Microbiol.* **2005**, *8*, 737−744.
(27) Soppa, J.; Oesterhelt, D. *J. Biol. Chem.* **1989**, *264*, 13043−13048.
(28) Soppa, J.; Oesterhelt, D. *J. Biol. Chem.* **1989**, *264*, 13049−13056.
(29) Haupts, U.; Tittor, J.; Bamberg, E.; Oesterhelt, D. *Biochemistry* **1997**, *36*, 2−7.
(30) Ferrando, E.; Schweiger, U.; Oesterhelt, D. *Gene* **1993**, *125*, 41−47.
(31) Pfeiffer, M.; Rink, T.; Gerwert, K.; Oesterhelt, D.; Steinhoff, H.-J. *J. Mol. Biol.* **1999**, *287*, 163−171.
(32) Knapp, H. F.; Mesquida, P.; Stemmer, A. *Surf. Interface Anal.* **2002**, *33*, 108−112.